Measuring Natural Frequency and Non-Linear Damping on Oscillating Micro Plates

Hartono Sumali Sandia National Laboratories MS 1070, PO Box 5800, Albuquerque, NM 87185, USA

ABSTRACT

This paper presents a method for measuring damping in single-degree-of-freedom oscillators where the natural frequency and damping ratios may vary with time, displacement, or velocity. The test structure was a micro plate suspended by folded springs. Response velocity was measured with a laser Doppler vibrometer and a microscope. Based on the Hilbert transform, a data processing technique was derived to calculate the damping ratio from time-domain free response data. The technique was applied to obtain damping ratios of the test structure from measurements under several different pressures. The result was linear damping ratio as a function of pressure, and a nonlinear part of damping as a function of velocity.

Nomenclature

A	Velocity amplitude, m/s	$\widetilde{\mathcal{v}}$	Hilbert transform of velocity, m/s
A_0	Initial amplitude, m/s	ϕ	Phase, rad
f_I	Fundamental natural frequency, Hz	τ	Decay time constant, s
$f_{\rm d}$	Damped oscillation frequency, Hz	ω	Frequency, rad/s
$f_{ m i}$	i th natural frequency, Hz Hilbert transform operator	ω_{d}	Damped oscillation frequency, rad/s
N	Number of time-domain data points	$\omega_{ m n}$	Natural frequency, rad/s
i	$\sqrt{-1}$	ζ	Damping ratio, dimensionless
t	Time, s	ζ lin	Linear damping ratio, dimensionless
V	Analytic representation of <i>v</i>	$\zeta_{ m nl}$	Non-linear damping ratio, dimensionless
ν	Velocity, m/s		

Introduction

Damping is very important in MEMS oscillators because it determines the quality factor and hence the resonant response. Thus, damping determines the quality of MEMS accelerometers, radio-frequency (RF) MEMS switches, MEMS gyroscopes, etc. Damping in MEMS is often dominated by squeeze film damping, which is much simpler to model and predict than damping caused by the solid structure. Hence, many damping models have been developed by other researchers and used widely for designing MEMS devices [1, 2]. However, measurement of damping in MEMS has not been done nearly as much as the modeling. Published measurements [3, 4] have not addressed the nonlinearity inherent to the variation of the thickness of the squeezed film gap throughout the oscillation cycle. This paper presents a method for measuring damping in MEMS. The test structure was a micro plate suspended by folded springs. Response velocity was measured with a laser Doppler vibrometer and a microscope. A technique was derived to calculate the damping ratio from measured velocities. The experiment was done under several different pressures.

The objective of the method is to obtain the natural frequency and damping of a single-degree-of-freedom (SDOF) oscillator, where the natural frequency and damping ratios may vary with time, displacement, or velocity.

Curve Fitting the Free Decaying Response

For an underdamped linear SDOF oscillator, the free decaying velocity response to an initial condition is

$$v_{lin}(t) = A_0 \exp(-\zeta \omega_n t) \cos(\omega_d t + \phi_0). \tag{1}$$

The decay rate

 ϕ_0

Initial phase, rad

$$1/\tau = \zeta \omega_{\rm p} \tag{2}$$

is a constant because both the damping ratio and the natural frequency are constant. If the damping ratio or the natural frequency is not constant, then the free decaying velocity response may be written as

$$v(t) = A_0 \exp(-t/\tau(t))\cos(\phi(t) + \phi_0). \tag{3}$$

Now the damped oscillation frequency

$$\omega_d(t) = \mathrm{d}\phi / \mathrm{d}t \tag{4}$$

may be time-varying. If the natural frequency ω_n is constant, then the damping ζ may be time-varying.

The measured free decay response data can be curve-fit to obtain the best linear estimate of $\zeta \omega_h$. The linear response can then be synthesized and subtracted form the measured response data to obtain the nonlinear response. That data processing method, based on the *Hilbert transform*, is described in the following.

The Hilbert transform of a signal v(t) is defined as

$$\widetilde{v}(t) = \mathcal{H}\{v(t)\} = \frac{1}{\pi} \int_{-\infty}^{\infty} \frac{v(\tau)}{t - \tau} d\tau , \qquad (5)$$

where the integral is evaluated as a Cauchy principal value to avoid singularities at $t=\tau$ and at $\tau=\pm\infty$. The analytic representation of the signal v(t) is defined as

$$V(t) = v(t) + j\widetilde{v}(t). \tag{6}$$

For the signal in Eq. (4), it can be shown that the magnitude of the analytic representation is the envelope of the signal, i.e.

$$|V| = A_0 \exp(-\zeta(t)\omega_n t). \tag{7}$$

Therefore, the decay rate $\zeta \omega_n$ can be obtained from the free decaying response v(t) measured at $t=t_0, t_1, ..., t_{N-1}$, by finding the least-squares solution to

$$\begin{cases}
\ln |V(t_0)| \\
\ln |V(t_1)| \\
\vdots \\
\ln |V(t_{N-1})|
\end{cases} = \begin{bmatrix} t_0 & 1 \\ t_1 & 1 \\ \vdots & \vdots \\ t_{N-1} & 1 \end{bmatrix} \begin{cases} \zeta \omega_n \\ \ln(A_0) \end{cases}, \tag{8}$$

which can be done easily using Matlab's left-matrix-divide operator.

For the signal in Eq. (4), it can also be shown that and the phase angle of the analytic representation is the phase of the signal, *i.e.*

$$\phi(t) + \phi_0 = \tan^{-1}(\widetilde{v}(t)/v(t)). \tag{9}$$

The damped oscillation frequency ω_d can be obtained from the above equation and time differentiation in Eq. (5). In practice, however, the noise introduced by the differentiation process can be greater than the resulting ω_d . A better way that avoids that noise is by finding the least-squares solution to

$$\begin{cases}
\tan^{-1}(\widetilde{v}(t_0)/v(t_0)) \\
\tan^{-1}(\widetilde{v}(t_1)/v(t_1)) \\
\vdots \\
\tan^{-1}(\widetilde{v}(t_{N-1})/v(t_{N-1}))
\end{cases} = \begin{bmatrix} t_0 & 1 \\ t_1 & 1 \\ \vdots & \vdots \\ t_{N-1} & 1 \end{bmatrix} \begin{bmatrix} \omega_{d} \\ \phi_{0} \end{bmatrix}.$$
(10)

Curve fitting in Eq. (9) gives $\zeta \omega_n$, the product of damping and natural frequency. Separating the damping ζ and undamped natural frequency ω_n is somewhat of a problem. For pure viscous damping, the value of the damped oscillation frequency from Eq. (11) could be used by virtue of the relationship

$$\omega_d = \omega_n \sqrt{1 - \zeta^2} \ . \tag{11}$$

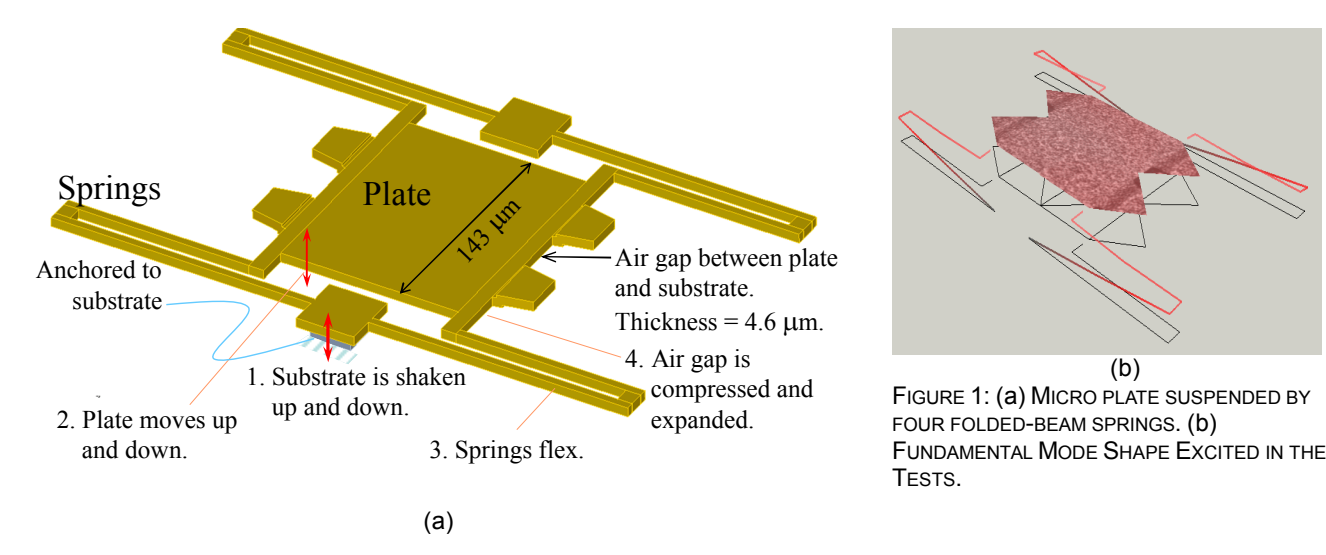
Unfortunately, for the case of squeeze-film damping, which often is the most important part of damping in MEMS oscillators, the above relationship does not hold. The squeezed fluid film gives extra stiffness to the structure. The damped oscillation frequency has been shown theoretically and experimentally to be higher than the undamped natural frequency, albeit slightly even for high damping. For that reason, an estimate is made that

$$\omega_{\rm n} \approx \omega_{\rm d}$$
. (12)

With the above estimate, the damping ratio ζ can be obtained after curve fitting in Eq. (8). The error will be a small fraction of the value of ζ .

Experiment

Figure 1(a) shows a solid model of the structure and how it was oscillated by the PZT shaker. The test structure consisted mainly of a plate suspended by four folded-beam springs. One end of each spring supports the plate; the other end is anchored to the substrate. The structures were made of electro-deposited gold. The width of the plate was $143\mu m$. A piezoelectric PZT transducer shook the substrate with vertical displacement. As a result, the plate oscillates vertically, expanding and squeezing the air layer between the plate and the substrate. The suspension springs flexed and provided restoring force to sustain the oscillation. The measured operational deflection shape in Fig. 1(b) shows that in the excited mode the plate oscillated vertically while staying parallel to the substrate. The experimental setup used for this testing is shown in Figure 2. A laser Doppler vibrometer (LDV) coupled with a microscope measured the velocity at the center of the plate. The spot size of the laser was about 1 μm . The test setup was enclosed in a vacuum chamber under air pressures from P=630Torr down to P<1mT=the resolution of the pressure gage.



Linear experimental modal analysis (EMA) had been done prior to the work discussed in this paper. The EMA was done with swept-sine base excitations from 1kHz to 200kHz, scanning seventeen points throughout the structure, in vacuum below 1mT. Modal parameter estimation using ME'ScopeTM gave natural frequencies of f_1 =16910Hz, f_2 =27240Hz, and f_3 =33050Hz. The

mode shapes are practically identical to the operational deflection shapes shown in Fig. 1(b) and Fig. (3). For the experiments discussed in this paper, the base excitation was a narrow-band burst chirp sweeping frequencies from f_1 -50Hz to f_1 +50Hz. The LDV measures the velocity of the center of the plate. That point is on the nodal lines where the two higher modes shown in Fig. 3 have zero or minimal contribution, even if they are excited at all. Each time-window starts with a buildup of the response from zero to a certain amplitude, at which time the burst excitation was turned off. The time window was long enough to ensure that the response died down below the noise floor at the end of each time window. With triggering precision of around 20nanoseconds, sixteen time windows were averaged to obtain the time-domain record of the plate velocity. The sampling rate was 1.28 Msamples/s. The number of points N was 65536 for most of the pressures. For high pressures where high damping decayed the response quickly, N was less.

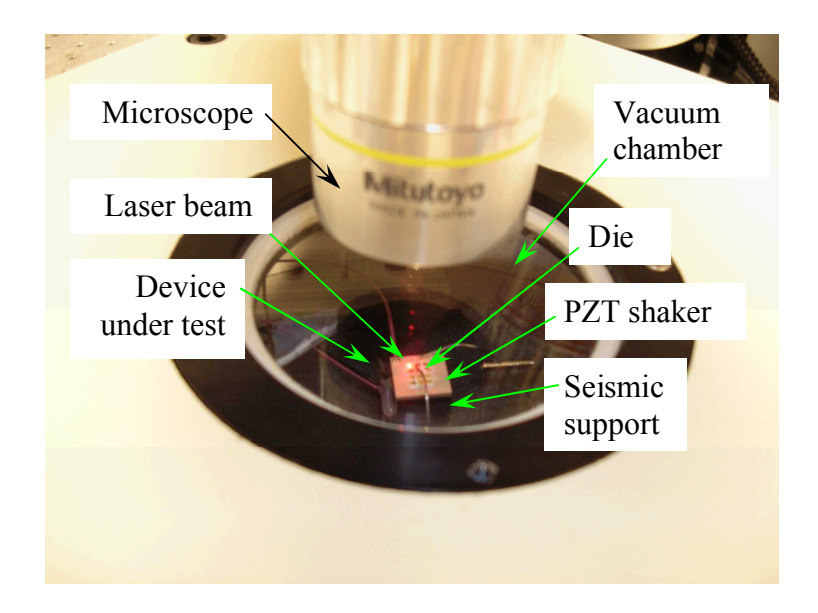
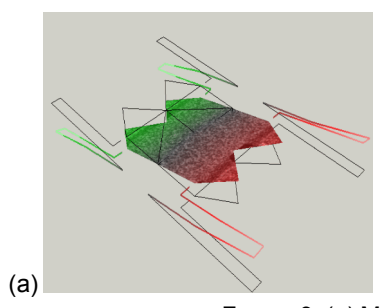


FIGURE 2: EXPERIMENT SETUP: THE STRUCTURE UNDER TEST WAS OSCILLATED BY SHAKING THE SUBSTRATE WITH A PZT SHAKER.



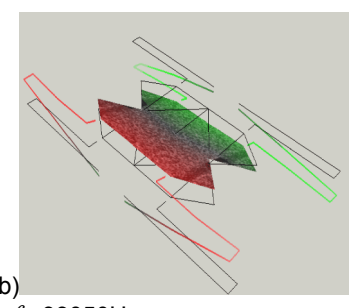


FIGURE 3: (a) MODE AT f_2 =27240Hz, (b) MODE AT f_3 =33050Hz

Application of the Method

The plate velocity measured at P=2.9Torr is shown in Fig. 4. The high number of cycles obviously prevents the figure to show the oscillations, but the figure does show the growing and then decaying envelope. To obtain the envelope function (Eq. (7)) that is not distorted by offset, drift and high-frequency noise, the velocity is filtered with a high-pass fourth-order Butterworth filter with a cutoff frequency of 6kHz, and a low-pass fourth-order Butterworth filter with a cutoff frequency of 200kHz. The discrete Fourier spectra in Fig. 5 show that the filtered velocity is practically the same as the raw velocity, but without the DC and low-frequency (drift) components. The spectra show a damped sinusoid with a peak at f_0 =16921Hz. (The frequency resolution is 25.218Hz.) The higher modes at f_0 =27240Hz, and f_0 =33050Hz did not contribute to the measured velocity. Harmonics at $2f_1$, $3f_0$, etc indicated that the oscillation might be non-linear.

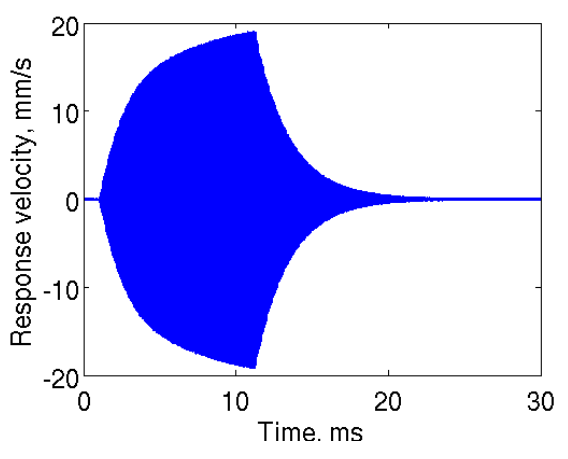


FIGURE 4: RESPONSE VELOCITY FOR 2.9TORR.

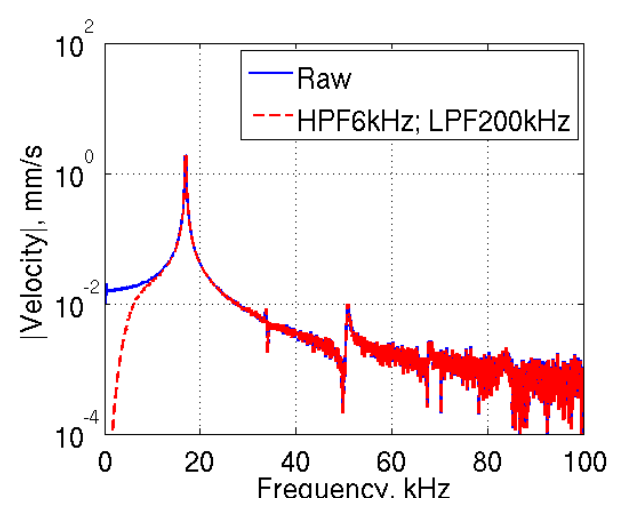


FIGURE 5: DISCRETE FOURIER SPECTRA OF RAW AND FILTERED RESPONSE VELOCITIES.

Figure 6 shows the analytic representation of the velocity signal, which is the real and imaginary parts of Eq. (6) and the envelope function from Eq. (7). The inset in that figure shows in detail the real part, the imaginary part, and the envelope, for a small portion of the graph indicated by the small box. The time axis has been shifted so that t=0 represents the start of the decay envelope. The phase angle of the analytic representation as obtained by Eq. (9) is shown with the solid line in the top graph in Fig. 7. Note that starting at around 15ms, the slope deviates rather grossly from the initial linear curve. Figure 6 shows that at that time the signal has died down, probably below the noise floor or instrument resolution. Recall that the oscillation frequency ω_d could be obtained by time-differentiation of the phase angle (Eq. (4)), or by least-squares linear fitting (Eq. (10)). The fit was done for t<15ms. The bottom graph in Fig. 7 demonstrates that the differentiation results in much higher noise than the least-squares fitting, at least for the data considered here. In fact, the plot is stopped at t=10ms to prevent the scaling from burying the detail. The log amplitude as a function of time is shown in Fig. 8. Curve-fitting in Eq. (8) results in the decay rate shown in Fig. 9. The fit appears very good. With the decay rate $\zeta \omega_n$ known, and the natural frequency ω_n obtained from Eq. (11), the damping ratio ζ is obtained and shown in Fig. 10 as a function of time. The mean of ζ is then taken as the estimate of the linear damping ratio ζ is obtained from that number is the component of the damping that varies with time, i.e.

$$\zeta_{nl} = \zeta - \zeta_{lin}. \tag{13}$$

Plotted against displacement in Fig. 11, ζ_{nl} does not seem to be a deterministic function of displacement. However, Fig. 12 suggests that ζ_{nl} may be a function of velocity.

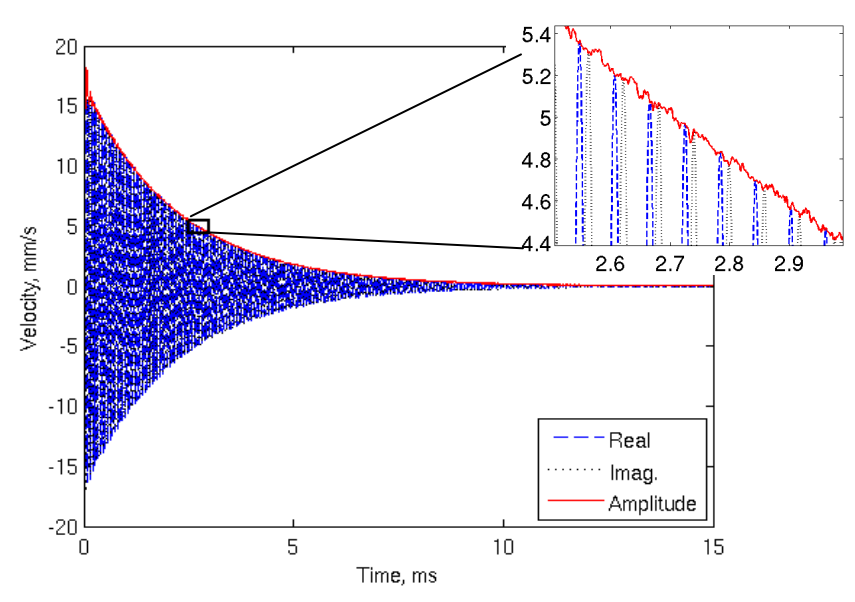


FIGURE 6: ANALYTIC REPRESENTATION OF THE FREE DECAYING VELOCITY.

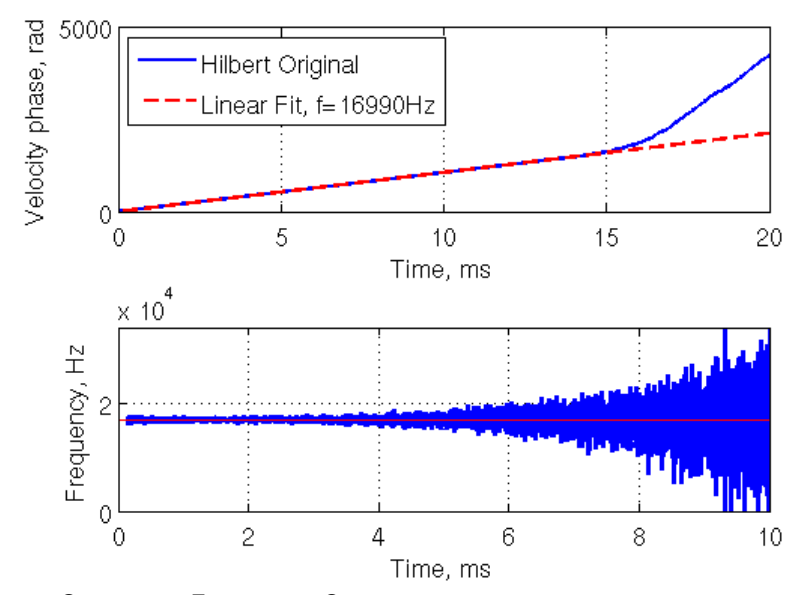
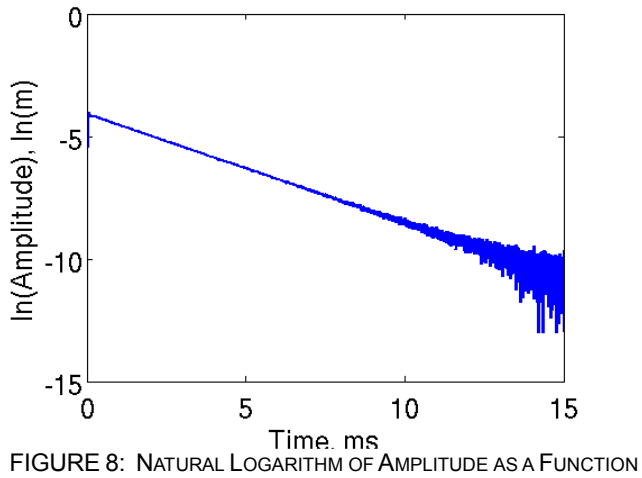


FIGURE 7: Phase Angle and Oscillation Frequency: Comparison between results of phase differentiation and of least-squares fitting.



OF TIME.

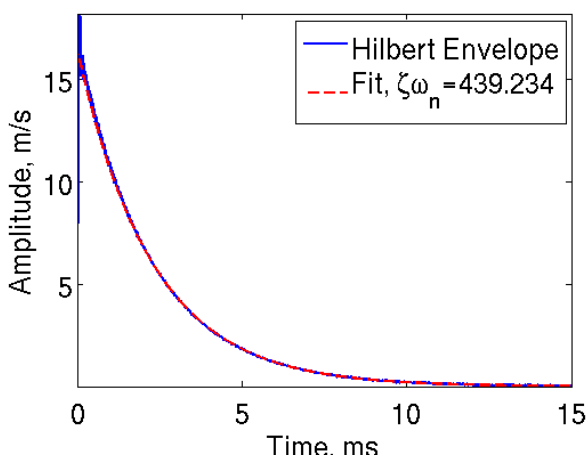
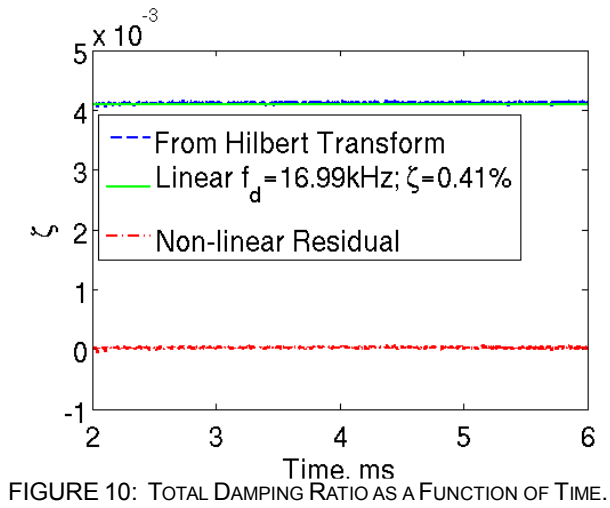


FIGURE 9: AMPLITUDE AS A FUNCTION OF TIME: FIT VALUES VERSUS MEASURED DATA.



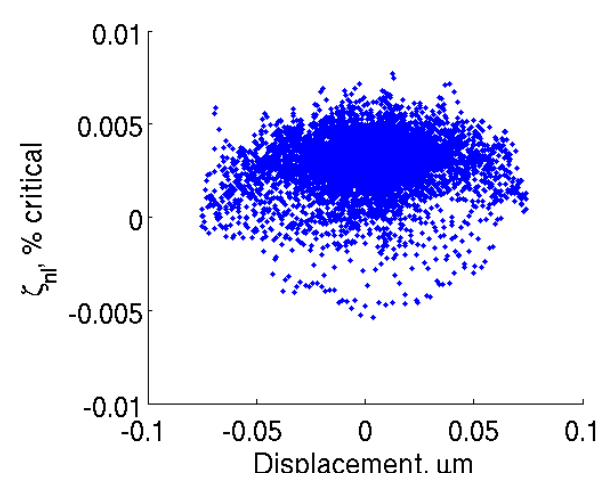


FIGURE 11: Nonlinear Damping Ratio versus Displacement.

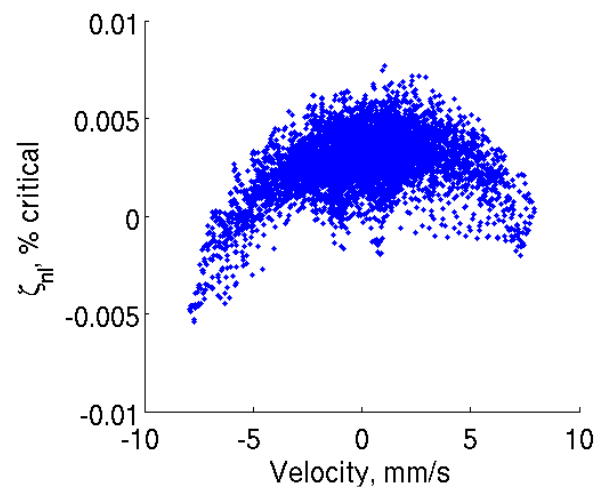


FIGURE 12: NONLINEAR DAMPING RATIO VERSUS VELOCITY.

Conclusions

The measurement and data processing technique resulted in accurate estimates of oscillation frequency and linear damping ratios. The damping ratio has been obtained as a function pressure, and can be used to check the damping models in the literature. The method reveals the nonlinear part of damping as a function of time, or phase in the oscillation cycle, which is related to velocity, displacement, and instantaneous thickness of the squeezed film between the plate and the substrate.

Acknowledgment

The author thanks Chris Dyck for the test structures. This work was conducted at Sandia National Laboratories. Sandia is a multi-program laboratory operated under Sandia Corporation, a Lockheed Martin Company, for the United States Department of Energy under Contract DE-AC04-94-AL85000.

References

- [1] Blech, J.J., 1983, "On Isothermal Squeeze Films", Journal of Lubrication Technology, 105, p 615-620.
- [2] Veijola, T., 2004, "Compact models for squeezed-film dampers with inertial and rarefied gas effects", *Journal of Micromechanics and Microengineering*, 14, p 1109-1118.
- [3] Andrews, M., Harris, I., Turner, G., 1993, "A comparison of squeeze-film theory with measurements on a microstructure", Sensors and Actuators A, 36, p 79-87.
- [4] Sumali, H., and Epp, D.S., 2006, "Squeeze Film Damping Models Compared with Tests on Microsystems", *Proc. 2005 ASME International Mechanical Engineering Congress and Exposition*, November 5-10, Chicago, IL.